

Measurements of neutral B decay branching fractions to $K_S^0 \pi^+ \pi^-$ final states and the charge asymmetry of $B^0 \rightarrow K^{*+} \pi^-$

B. Aubert,¹ R. Barate,¹ D. Boutigny,¹ F. Couderc,¹ Y. Karyotakis,¹ J. P. Lees,¹ V. Poireau,¹ V. Tisserand,¹ A. Zghiche,¹ E. Grauges,² A. Palano,³ M. Pappagallo,³ A. Pompili,³ J. C. Chen,⁴ N. D. Qi,⁴ G. Rong,⁴ P. Wang,⁴ Y. S. Zhu,⁴ G. Eigen,⁵ I. Ofte,⁵ B. Stugu,⁵ G. S. Abrams,⁶ M. Battaglia,⁶ A. B. Breon,⁶ D. N. Brown,⁶ J. Button-Shafer,⁶ R. N. Cahn,⁶ E. Charles,⁶ C. T. Day,⁶ M. S. Gill,⁶ A. V. Gritsan,⁶ Y. Groysman,⁶ R. G. Jacobsen,⁶ R. W. Kadel,⁶ J. Kadyk,⁶ L. T. Kerth,⁶ Yu. G. Kolomensky,⁶ G. Kukartsev,⁶ G. Lynch,⁶ L. M. Mir,⁶ P. J. Oddone,⁶ T. J. Orimoto,⁶ M. Pripstein,⁶ N. A. Roe,⁶ M. T. Ronan,⁶ W. A. Wenzel,⁶ M. Barrett,⁷ K. E. Ford,⁷ T. J. Harrison,⁷ A. J. Hart,⁷ C. M. Hawkes,⁷ S. E. Morgan,⁷ A. T. Watson,⁷ M. Fritsch,⁸ K. Goetzen,⁸ T. Held,⁸ H. Koch,⁸ B. Lewandowski,⁸ M. Pelizaeus,⁸ K. Peters,⁸ T. Schroeder,⁸ M. Steinke,⁸ J. T. Boyd,⁹ J. P. Burke,⁹ N. Chevalier,⁹ W. N. Cottingham,⁹ T. Cuhadar-Donszelmann,¹⁰ B. G. Fulsom,¹⁰ C. Hearty,¹⁰ N. S. Knecht,¹⁰ T. S. Mattison,¹⁰ J. A. McKenna,¹⁰ A. Khan,¹¹ P. Kyberd,¹¹ M. Saleem,¹¹ L. Teodorescu,¹¹ A. E. Blinov,¹² V. E. Blinov,¹² A. D. Bukin,¹² V. P. Druzhinin,¹² V. B. Golubev,¹² E. A. Kravchenko,¹² A. P. Onuchin,¹² S. I. Serednyakov,¹² Yu. I. Skovpen,¹² E. P. Solodov,¹² A. N. Yushkov,¹² D. Best,¹³ M. Bondioli,¹³ M. Bruinsma,¹³ M. Chao,¹³ S. Curry,¹³ I. Eschrich,¹³ D. Kirkby,¹³ A. J. Lankford,¹³ P. Lund,¹³ M. Mandelkern,¹³ R. K. Mommsen,¹³ W. Roethel,¹³ D. P. Stoker,¹³ C. Buchanan,¹⁴ B. L. Hartfiel,¹⁴ A. J. R. Weinstein,¹⁴ S. D. Foulkes,¹⁵ J. W. Gary,¹⁵ O. Long,¹⁵ B. C. Shen,¹⁵ K. Wang,¹⁵ L. Zhang,¹⁵ D. del Re,¹⁶ H. K. Hadavand,¹⁶ E. J. Hill,¹⁶ D. B. MacFarlane,¹⁶ H. P. Paar,¹⁶ S. Rahatlou,¹⁶ V. Sharma,¹⁶ J. W. Berryhill,¹⁷ C. Campagnari,¹⁷ A. Cunha,¹⁷ B. Dahmes,¹⁷ T. M. Hong,¹⁷ M. A. Mazur,¹⁷ J. D. Richman,¹⁷ W. Verkerke,¹⁷ T. W. Beck,¹⁸ A. M. Eisner,¹⁸ C. J. Flacco,¹⁸ C. A. Heusch,¹⁸ J. Kroseberg,¹⁸ W. S. Lockman,¹⁸ G. Nesom,¹⁸ T. Schalk,¹⁸ B. A. Schumm,¹⁸ A. Seiden,¹⁸ P. Spradlin,¹⁸ D. C. Williams,¹⁸ M. G. Wilson,¹⁸ J. Albert,¹⁹ E. Chen,¹⁹ G. P. Dubois-Felsmann,¹⁹ A. Dvoretzki,¹⁹ D. G. Hitlin,¹⁹ I. Narsky,¹⁹ T. Piatenko,¹⁹ F. C. Porter,¹⁹ A. Ryd,¹⁹ A. Samuel,¹⁹ R. Andreassen,²⁰ S. Jayatilake,²⁰ G. Mancinelli,²⁰ B. T. Meadows,²⁰ M. D. Sokoloff,²⁰ F. Blanc,²¹ P. Bloom,²¹ S. Chen,²¹ W. T. Ford,²¹ J. F. Hirschauer,²¹ A. Kreisel,²¹ U. Nauenberg,²¹ A. Olivas,²¹ P. Rankin,²¹ W. O. Ruddick,²¹ J. G. Smith,²¹ K. A. Ulmer,²¹ S. R. Wagner,²¹ J. Zhang,²¹ A. Chen,²² E. A. Eckhart,²² A. Soffer,²² W. H. Toki,²² R. J. Wilson,²² Q. Zeng,²² D. Altenburg,²³ E. Feltresi,²³ A. Hauke,²³ B. Spaan,²³ T. Brandt,²⁴ J. Brose,²⁴ M. Dickopp,²⁴ V. Klose,²⁴ H. M. Lacker,²⁴ R. Nogowski,²⁴ S. Otto,²⁴ A. Petzold,²⁴ G. Schott,²⁴ J. Schubert,²⁴ K. R. Schubert,²⁴ R. Schwierz,²⁴ J. E. Sundermann,²⁴ D. Bernard,²⁵ G. R. Bonneaud,²⁵ P. Grenier,²⁵ S. Schrenk,²⁵ Ch. Thiebaux,²⁵ G. Vasileiadis,²⁵ M. Verderi,²⁵ D. J. Bard,²⁶ P. J. Clark,²⁶ W. Gradl,²⁶ F. Muheim,²⁶ S. Playfer,²⁶ Y. Xie,²⁶ M. Andreotti,²⁷ V. Azzolini,²⁷ D. Bettoni,²⁷ C. Bozzi,²⁷ R. Calabrese,²⁷ G. Cibinetto,²⁷ E. Luppi,²⁷ M. Negri,²⁷ L. Piemontese,²⁷ F. Anulli,²⁸ R. Baldini-Ferrolli,²⁸ A. Calcaterra,²⁸ R. de Sangro,²⁸ G. Finocchiaro,²⁸ P. Patteri,²⁸ I. M. Peruzzi,^{28,*} M. Piccolo,²⁸ A. Zallo,²⁸ A. Buzzo,²⁹ R. Capra,²⁹ R. Contri,²⁹ M. Lo Vetere,²⁹ M. Macri,²⁹ M. R. Monge,²⁹ S. Passaggio,²⁹ C. Patrignani,²⁹ E. Robutti,²⁹ A. Santroni,²⁹ S. Tosi,²⁹ G. Brandenburg,³⁰ K. S. Chaisanguanthum,³⁰ M. Morii,³⁰ E. Won,³⁰ J. Wu,³⁰ R. S. Dubitzky,³¹ U. Langenegger,³¹ J. Marks,³¹ S. Schenk,³¹ U. Uwer,³¹ W. Bhimji,³² D. A. Bowerman,³² P. D. Dauncey,³² U. Egede,³² R. L. Flack,³² J. R. Gaillard,³² G. W. Morton,³² J. A. Nash,³² M. B. Nikolich,³² G. P. Taylor,³² W. P. Vazquez,³² M. J. Charles,³³ W. F. Mader,³³ U. Mallik,³³ A. K. Mohapatra,³³ J. Cochran,³⁴ H. B. Crawley,³⁴ V. Eyges,³⁴ W. T. Meyer,³⁴ S. Prell,³⁴ E. I. Rosenberg,³⁴ A. E. Rubin,³⁴ J. Yi,³⁴ N. Arnaud,³⁵ M. Davier,³⁵ X. Giroux,³⁵ G. Grosdidier,³⁵ A. Höcker,³⁵ F. Le Diberder,³⁵ V. Lepeltier,³⁵ A. M. Lutz,³⁵ A. Oyanguren,³⁵ T. C. Petersen,³⁵ M. Pierini,³⁵ S. Plaszczynski,³⁵ S. Rodier,³⁵ P. Roudeau,³⁵ M. H. Schune,³⁵ A. Stocchi,³⁵ G. Wormser,³⁵ C. H. Cheng,³⁶ D. J. Lange,³⁶ M. C. Simani,³⁶ D. M. Wright,³⁶ A. J. Bevan,³⁷ C. A. Chavez,³⁷ I. J. Forster,³⁷ J. R. Fry,³⁷ E. Gabathuler,³⁷ R. Gamet,³⁷ K. A. George,³⁷ D. E. Hutchcroft,³⁷ R. J. Parry,³⁷ D. J. Payne,³⁷ K. C. Schofield,³⁷ C. Touramanis,³⁷ C. M. Cormack,³⁸ F. Di Lodovico,³⁸ W. Menges,³⁸ R. Sacco,³⁸ C. L. Brown,³⁹ G. Cowan,³⁹ H. U. Flaecher,³⁹ M. G. Green,³⁹ D. A. Hopkins,³⁹ P. S. Jackson,³⁹ T. R. McMahon,³⁹ S. Ricciardi,³⁹ F. Salvatore,³⁹ D. Brown,⁴⁰ C. L. Davis,⁴⁰ J. Allison,⁴¹ N. R. Barlow,⁴¹ R. J. Barlow,⁴¹ C. L. Edgar,⁴¹ M. C. Hodgkinson,⁴¹ M. P. Kelly,⁴¹ G. D. Lafferty,⁴¹ M. T. Naisbit,⁴¹ J. C. Williams,⁴¹ C. Chen,⁴² W. D. Hulsbergen,⁴² A. Jawahery,⁴² D. Kovalskiy,⁴² C. K. Lae,⁴² D. A. Roberts,⁴² G. Simi,⁴² G. Blaylock,⁴³ C. Dallapiccola,⁴³ S. S. Hertzbach,⁴³ R. Kofler,⁴³ V. B. Koptchev,⁴³ X. Li,⁴³ T. B. Moore,⁴³ S. Saremi,⁴³ H. Staengle,⁴³ S. Willocq,⁴³ R. Cowan,⁴⁴ K. Koeneke,⁴⁴ G. Sciolla,⁴⁴ S. J. Sekula,⁴⁴ M. Spitznagel,⁴⁴ F. Taylor,⁴⁴ R. K. Yamamoto,⁴⁴ H. Kim,⁴⁵ P. M. Patel,⁴⁵ S. H. Robertson,⁴⁵ A. Lazzaro,⁴⁶ V. Lombardo,⁴⁶ F. Palombo,⁴⁶ J. M. Bauer,⁴⁷ L. Cremaldi,⁴⁷ V. Eschenburg,⁴⁷ R. Godang,⁴⁷ R. Kroeger,⁴⁷ J. Reidy,⁴⁷ D. A. Sanders,⁴⁷ D. J. Summers,⁴⁷ H. W. Zhao,⁴⁷ S. Brunet,⁴⁸ D. Côté,⁴⁸ P. Taras,⁴⁸ B. Viaud,⁴⁸ H. Nicholson,⁴⁹ N. Cavallo,^{50,†} G. De Nardo,⁵⁰ F. Fabozzi,^{50,†} C. Gatto,⁵⁰ L. Lista,⁵⁰ D. Monorchio,⁵⁰ P. Paolucci,⁵⁰ D. Piccolo,⁵⁰ C. Sciacca,⁵⁰ M. Baak,⁵¹ H. Bulten,⁵¹ G. Raven,⁵¹ H. L. Snoek,⁵¹ L. Wilden,⁵¹ C. P. Jessop,⁵² J. M. LoSecco,⁵²

T. Allmendinger,⁵³ G. Benelli,⁵³ K. K. Gan,⁵³ K. Honscheid,⁵³ D. Hufnagel,⁵³ P. D. Jackson,⁵³ H. Kagan,⁵³ R. Kass,⁵³ T. Pulliam,⁵³ A. M. Rahimi,⁵³ R. Ter-Antonyan,⁵³ Q. K. Wong,⁵³ J. Brau,⁵⁴ R. Frey,⁵⁴ O. Igonkina,⁵⁴ M. Lu,⁵⁴ C. T. Potter,⁵⁴ N. B. Sinev,⁵⁴ D. Strom,⁵⁴ J. Strube,⁵⁴ E. Torrence,⁵⁴ F. Galeazzi,⁵⁵ M. Margoni,⁵⁵ M. Morandin,⁵⁵ M. Posocco,⁵⁵ M. Rotondo,⁵⁵ F. Simonetto,⁵⁵ R. Stroili,⁵⁵ C. Voci,⁵⁵ M. Benayoun,⁵⁶ H. Briand,⁵⁶ J. Chauveau,⁵⁶ P. David,⁵⁶ L. Del Buono,⁵⁶ Ch. de la Vaissière,⁵⁶ O. Hamon,⁵⁶ M. J. J. John,⁵⁶ Ph. Leruste,⁵⁶ J. Malclès,⁵⁶ J. Ocariz,⁵⁶ L. Roos,⁵⁶ G. Therin,⁵⁶ P. K. Behera,⁵⁷ L. Gladney,⁵⁷ Q. H. Guo,⁵⁷ J. Panetta,⁵⁷ M. Biasini,⁵⁸ R. Covarelli,⁵⁸ S. Pacetti,⁵⁸ M. Pioppi,⁵⁸ C. Angelini,⁵⁹ G. Batignani,⁵⁹ S. Bettarini,⁵⁹ F. Bucci,⁵⁹ G. Calderini,⁵⁹ M. Carpinelli,⁵⁹ R. Cenci,⁵⁹ F. Forti,⁵⁹ M. A. Giorgi,⁵⁹ A. Lusiani,⁵⁹ G. Marchiori,⁵⁹ M. Morganti,⁵⁹ N. Neri,⁵⁹ E. Paoloni,⁵⁹ M. Rama,⁵⁹ G. Rizzo,⁵⁹ J. Walsh,⁵⁹ M. Haire,⁶⁰ D. Judd,⁶⁰ D. E. Wagoner,⁶⁰ J. Biesiada,⁶¹ N. Danielson,⁶¹ P. Elmer,⁶¹ Y. P. Lau,⁶¹ C. Lu,⁶¹ J. Olsen,⁶¹ A. J. S. Smith,⁶¹ A. V. Telnov,⁶¹ F. Bellini,⁶² G. Cavoto,⁶² A. D’Orazio,⁶² E. Di Marco,⁶² R. Faccini,⁶² F. Ferrarotto,⁶² F. Ferroni,⁶² M. Gaspero,⁶² L. Li Gioi,⁶² M. A. Mazzoni,⁶² S. Morganti,⁶² G. Piredda,⁶² F. Polci,⁶² F. Safai Tehrani,⁶² C. Voena,⁶² H. Schröder,⁶³ G. Wagner,⁶³ R. Waldi,⁶³ T. Adye,⁶⁴ N. De Groot,⁶⁴ B. Franek,⁶⁴ G. P. Gopal,⁶⁴ E. O. Olaiya,⁶⁴ F. F. Wilson,⁶⁴ R. Aleksan,⁶⁵ S. Emery,⁶⁵ A. Gaidot,⁶⁵ S. F. Ganzhur,⁶⁵ P.-F. Giraud,⁶⁵ G. Graziani,⁶⁵ G. Hamel de Monchenault,⁶⁵ W. Kozanecki,⁶⁵ M. Legendre,⁶⁵ G. W. London,⁶⁵ B. Mayer,⁶⁵ G. Vasseur,⁶⁵ Ch. Yèche,⁶⁵ M. Zito,⁶⁵ M. V. Purohit,⁶⁶ A. W. Weidemann,⁶⁶ J. R. Wilson,⁶⁶ F. X. Yumiceva,⁶⁶ T. Abe,⁶⁷ M. T. Allen,⁶⁷ D. Aston,⁶⁷ N. van Bakel,⁶⁷ R. Bartoldus,⁶⁷ N. Berger,⁶⁷ A. M. Boyarski,⁶⁷ O. L. Buchmueller,⁶⁷ R. Claus,⁶⁷ J. P. Coleman,⁶⁷ M. R. Convery,⁶⁷ M. Cristinziani,⁶⁷ J. C. Dingfelder,⁶⁷ D. Dong,⁶⁷ J. Dorfan,⁶⁷ D. Dujmic,⁶⁷ W. Dunwoodie,⁶⁷ S. Fan,⁶⁷ R. C. Field,⁶⁷ T. Glanzman,⁶⁷ S. J. Gowdy,⁶⁷ T. Hadig,⁶⁷ V. Halyo,⁶⁷ C. Hast,⁶⁷ T. Hryn’ova,⁶⁷ W. R. Innes,⁶⁷ M. H. Kelsey,⁶⁷ P. Kim,⁶⁷ M. L. Kocian,⁶⁷ D. W. G. S. Leith,⁶⁷ J. Libby,⁶⁷ S. Luitz,⁶⁷ V. Luth,⁶⁷ H. L. Lynch,⁶⁷ H. Marsiske,⁶⁷ R. Messner,⁶⁷ D. R. Muller,⁶⁷ C. P. O’Grady,⁶⁷ V. E. Ozcan,⁶⁷ A. Perazzo,⁶⁷ M. Perl,⁶⁷ B. N. Ratcliff,⁶⁷ A. Roodman,⁶⁷ A. A. Salnikov,⁶⁷ R. H. Schindler,⁶⁷ J. Schwiening,⁶⁷ A. Snyder,⁶⁷ J. Stelzer,⁶⁷ D. Su,⁶⁷ M. K. Sullivan,⁶⁷ K. Suzuki,⁶⁷ S. Swain,⁶⁷ J. M. Thompson,⁶⁷ J. Va’vra,⁶⁷ M. Weaver,⁶⁷ W. J. Wisniewski,⁶⁷ M. Wittgen,⁶⁷ D. H. Wright,⁶⁷ A. K. Yarritu,⁶⁷ K. Yi,⁶⁷ C. C. Young,⁶⁷ P. R. Burchat,⁶⁸ A. J. Edwards,⁶⁸ S. A. Majewski,⁶⁸ B. A. Petersen,⁶⁸ C. Roat,⁶⁸ M. Ahmed,⁶⁹ S. Ahmed,⁶⁹ M. S. Alam,⁶⁹ J. A. Ernst,⁶⁹ M. A. Saeed,⁶⁹ F. R. Wappler,⁶⁹ S. B. Zain,⁶⁹ W. Bugg,⁷⁰ M. Krishnamurthy,⁷⁰ S. M. Spanier,⁷⁰ R. Eckmann,⁷¹ J. L. Ritchie,⁷¹ A. Satpathy,⁷¹ R. F. Schwitters,⁷¹ J. M. Izen,⁷² I. Kitayama,⁷² X. C. Lou,⁷² S. Ye,⁷² F. Bianchi,⁷³ M. Bona,⁷³ F. Gallo,⁷³ D. Gamba,⁷³ M. Bomben,⁷⁴ L. Bosisio,⁷⁴ C. Cartaro,⁷⁴ F. Cossutti,⁷⁴ G. Della Ricca,⁷⁴ S. Dittongo,⁷⁴ S. Grancagnolo,⁷⁴ L. Lanceri,⁷⁴ L. Vitale,⁷⁴ F. Martinez-Vidal,⁷⁵ R. S. Panvini,^{76,‡} Sw. Banerjee,⁷⁷ B. Bhuyan,⁷⁷ C. M. Brown,⁷⁷ D. Fortin,⁷⁷ K. Hamano,⁷⁷ R. Kowalewski,⁷⁷ J. M. Roney,⁷⁷ R. J. Sobie,⁷⁷ J. J. Back,⁷⁸ P. F. Harrison,⁷⁸ T. E. Latham,⁷⁸ G. B. Mohanty,⁷⁸ H. R. Band,⁷⁹ X. Chen,⁷⁹ B. Cheng,⁷⁹ S. Dasu,⁷⁹ M. Datta,⁷⁹ A. M. Eichenbaum,⁷⁹ K. T. Flood,⁷⁹ M. Graham,⁷⁹ J. J. Hollar,⁷⁹ J. R. Johnson,⁷⁹ P. E. Kutter,⁷⁹ H. Li,⁷⁹ R. Liu,⁷⁹ B. Mellado,⁷⁹ A. Mihalyi,⁷⁹ Y. Pan,⁷⁹ R. Prepost,⁷⁹ P. Tan,⁷⁹ J. H. von Wimmersperg-Toeller,⁷⁹ S. L. Wu,⁷⁹ Z. Yu,⁷⁹ and H. Neal⁸⁰

(BABAR Collaboration)

¹Laboratoire de Physique des Particules, F-74941 Annecy-le-Vieux, France

²IFAE, Universitat Autònoma de Barcelona, E-08193 Bellaterra, Barcelona, Spain

³Università di Bari, Dipartimento di Fisica and INFN, I-70126 Bari, Italy

⁴Institute of High Energy Physics, Beijing 100039, China

⁵Inst. of Physics, University of Bergen, N-5007 Bergen, Norway

⁶Lawrence Berkeley National Laboratory and University of California, Berkeley, California 94720, USA

⁷University of Birmingham, Birmingham, B15 2TT, United Kingdom

⁸Institut für Experimentalphysik, Ruhr Universität Bochum, I, D-44780 Bochum, Germany

⁹University of Bristol, Bristol BS8 1TL, United Kingdom

¹⁰University of British Columbia, Vancouver, British Columbia, Canada V6T 1Z1

¹¹Brunel University, Uxbridge, Middlesex UB8 3PH, United Kingdom

¹²Budker Institute of Nuclear Physics, Novosibirsk 630090, Russia

¹³University of California at Irvine, Irvine, California 92697, USA

¹⁴University of California at Los Angeles, Los Angeles, California 90024, USA

¹⁵University of California at Riverside, Riverside, California 92521, USA

¹⁶University of California at San Diego, La Jolla, California 92093, USA

¹⁷University of California at Santa Barbara, Santa Barbara, California 93106, USA

¹⁸University of California at Santa Cruz, Institute for Particle Physics, Santa Cruz, California 95064, USA

¹⁹California Institute of Technology, Pasadena, California 91125, USA

- ²⁰University of Cincinnati, Cincinnati, Ohio 45221, USA
²¹University of Colorado, Boulder, Colorado 80309, USA
²²Colorado State University, Fort Collins, Colorado 80523, USA
²³Institut für Physik, Universität Dortmund, D-44221 Dortmund, Germany
²⁴Institut für Kern- und Teilchenphysik, Technische Universität Dresden, D-01062 Dresden, Germany
²⁵Ecole Polytechnique, LLR, F-91128 Palaiseau, France
²⁶University of Edinburgh, Edinburgh EH9 3JZ, United Kingdom
²⁷Dipartimento di Fisica and INFN, Università di Ferrara, I-44100 Ferrara, Italy
²⁸Laboratori Nazionali di Frascati dell'INFN, I-00044 Frascati, Italy
²⁹Dipartimento di Fisica and INFN, Università di Genova, I-16146 Genova, Italy
³⁰Harvard University, Cambridge, Massachusetts 02138, USA
³¹Physikalisches Institut, Universität Heidelberg, Philosophenweg 12, D-69120 Heidelberg, Germany
³²Imperial College London, London, SW7 2AZ, United Kingdom
³³University of Iowa, Iowa City, Iowa 52242, USA
³⁴Iowa State University, Ames, Iowa 50011-3160, USA
³⁵Laboratoire de l'Accélérateur Linéaire, F-91898 Orsay, France
³⁶Lawrence Livermore National Laboratory, Livermore, California 94550, USA
³⁷University of Liverpool, Liverpool L69 7ZE, United Kingdom
³⁸Queen Mary, University of London, E1 4NS, United Kingdom
³⁹University of London, Royal Holloway and Bedford New College, Egham, Surrey TW20 0EX, United Kingdom
⁴⁰University of Louisville, Louisville, Kentucky 40292, USA
⁴¹University of Manchester, Manchester M13 9PL, United Kingdom
⁴²University of Maryland, College Park, Maryland 20742, USA
⁴³University of Massachusetts, Amherst, Massachusetts 01003, USA
⁴⁴Laboratory for Nuclear Science, Massachusetts Institute of Technology, Cambridge, Massachusetts 02139, USA
⁴⁵McGill University, Montréal, Quebec, Canada H3A 2T8
⁴⁶Dipartimento di Fisica and INFN, Università di Milano, I-20133 Milano, Italy
⁴⁷University of Mississippi, University, Mississippi 38677, USA
⁴⁸Université de Montréal, Laboratoire René J. A. Lévesque, Montréal, Quebec, Canada H3C 3J7
⁴⁹Mount Holyoke College, South Hadley, Massachusetts 01075, USA
⁵⁰Dipartimento di Scienze Fisiche and INFN, Università di Napoli Federico II, I-80126, Napoli, Italy
⁵¹NIKHEF, National Institute for Nuclear Physics and High Energy Physics, NL-1009 DB Amsterdam, The Netherlands
⁵²University of Notre Dame, Notre Dame, Indiana 46556, USA
⁵³Ohio State University, Columbus, Ohio 43210, USA
⁵⁴University of Oregon, Eugene, Oregon 97403, USA
⁵⁵Dipartimento di Fisica and INFN, Università di Padova, I-35131 Padova, Italy
⁵⁶Laboratoire de Physique Nucléaire et de Hautes Energies, Universités Paris VI et VII, F-75252 Paris, France
⁵⁷University of Pennsylvania, Philadelphia, Pennsylvania 19104, USA
⁵⁸Dipartimento di Fisica and INFN, Università di Perugia, I-06100 Perugia, Italy
⁵⁹Dipartimento di Fisica, Scuola Normale Superiore and INFN, Università di Pisa, I-56127 Pisa, Italy
⁶⁰Prairie View A&M University, Prairie View, Texas 77446, USA
⁶¹Princeton University, Princeton, New Jersey 08544, USA
⁶²Dipartimento di Fisica and INFN, Università di Roma La Sapienza, I-00185 Roma, Italy
⁶³Universität Rostock, D-18051 Rostock, Germany
⁶⁴Rutherford Appleton Laboratory, Chilton, Didcot, Oxon, OX11 0QX, United Kingdom
⁶⁵DSM/Dapnia, CEA/Saclay, F-91191 Gif-sur-Yvette, France
⁶⁶University of South Carolina, Columbia, South Carolina 29208, USA
⁶⁷Stanford Linear Accelerator Center, Stanford, California 94309, USA
⁶⁸Stanford University, Stanford, California 94305-4060, USA
⁶⁹State University of New York, Albany, New York 12222, USA
⁷⁰University of Tennessee, Knoxville, Tennessee 37996, USA
⁷¹University of Texas at Austin, Austin, Texas 78712, USA
⁷²Dipartimento di Fisica Sperimentale and INFN, University of Texas at Dallas, Richardson, Texas 75083, USA
⁷³Università di Torino, I-10125 Torino, Italy
⁷⁴Dipartimento di Fisica and INFN, Università di Trieste, I-34127 Trieste, Italy
⁷⁵IFIC, Universitat de Valencia-CSIC, E-46071 Valencia, Spain

* Also with Università di Perugia, Dipartimento di Fisica, Perugia, Italy

† Also with Università della Basilicata, Potenza, Italy

‡ Deceased

⁷⁶Vanderbilt University, Nashville, Tennessee 37235, USA⁷⁷University of Victoria, Victoria, British Columbia, Canada V8W 3P6⁷⁸Department of Physics, University of Warwick, Coventry CV4 7AL, United Kingdom⁷⁹University of Wisconsin, Madison, Wisconsin 53706, USA⁸⁰Yale University, New Haven, Connecticut 06511, USA

(Received 4 August 2005; published 15 February 2006)

We analyze the decay $B^0 \rightarrow K_S^0 \pi^+ \pi^-$ using a sample of 232×10^6 $Y(4S) \rightarrow B\bar{B}$ decays collected with the *BABAR* detector at the SLAC PEP-II asymmetric-energy B factory. A maximum likelihood fit finds the following branching fractions: $\mathcal{B}(B^0 \rightarrow K^0 \pi^+ \pi^-) = (43.0 \pm 2.3 \pm 2.3) \times 10^{-6}$, $\mathcal{B}(B^0 \rightarrow f_0(\rightarrow \pi^+ \pi^-) K^0) = (5.5 \pm 0.7 \pm 0.5 \pm 0.3) \times 10^{-6}$ and $\mathcal{B}(B^0 \rightarrow K^{*+} \pi^-) = (11.0 \pm 1.5 \pm 0.5 \pm 0.5) \times 10^{-6}$. For these results, the first uncertainty is statistical, the second is systematic, and the third (if present) is due to the effect of interference from other resonances. We also measure the CP -violating charge asymmetry in the decay $B^0 \rightarrow K^{*+} \pi^-$, $\mathcal{A}_{K^* \pi} = -0.11 \pm 0.14 \pm 0.05$.

DOI: [10.1103/PhysRevD.73.031101](https://doi.org/10.1103/PhysRevD.73.031101)

PACS numbers: 13.25.Hw, 11.30.Er, 12.15.Hh

Measurements of charmless three-body B decays, which are dominated by their intermediate quasi-two-body decays, are important in furthering our understanding of quark couplings described by the Cabibbo-Kobayashi-Maskawa matrix [1]. CP violation can be probed through the investigation of neutral B -meson decays to resonance channels with the final state $K_S^0 \pi^+ \pi^-$, such as $f_0 K_S^0$ [2], $\rho^0 K_S^0$ [3] and $K^{*+} \pi^-$ [4].

By measuring the charmless branching fraction of $B^0 \rightarrow K_S^0 \pi^+ \pi^-$, along with those of its dominant resonant submodes, we can obtain information about the structure of the decay Dalitz plot. Such measurements have previously been performed by the CLEO [5], Belle [6] and *BABAR* [2–4] experiments.

QCD factorization models [7] have predicted branching fractions and asymmetries for charmless B decays. Predictions have also been made using flavor SU(3) symmetry [8]. For $B^0 \rightarrow K^{*+} \pi^-$, predictions [9] have been made for the branching fractions and charge asymmetry,

$$\mathcal{A}_{K^* \pi} = \frac{\Gamma_{\bar{B}^0 \rightarrow K^{*-} \pi^+} - \Gamma_{B^0 \rightarrow K^{*+} \pi^-}}{\Gamma_{\bar{B}^0 \rightarrow K^{*-} \pi^+} + \Gamma_{B^0 \rightarrow K^{*+} \pi^-}}, \quad (1)$$

which is a CP -violating quantity since the decay channel is a flavor eigenstate. CP violation in charge asymmetry has already been observed by *BABAR* and Belle in $B^0 \rightarrow K^+ \pi^-$ [10].

In this paper the branching fractions of $B^0 \rightarrow K^0 \pi^+ \pi^-$, $B^0 \rightarrow K^{*+} \pi^-$ and $B^0 \rightarrow f_0(980)(\rightarrow \pi^+ \pi^-) K^0$ are presented, averaged over charge-conjugate states, along with a measurement of the charge asymmetry in $B^0 \rightarrow K^{*+} \pi^-$. The selection criteria require events with a reconstructed K_S^0 in the final state. Results are stated in terms of the K^0 final state, taking into account the probabilities for $\mathcal{B}(K^0 \rightarrow K_S^0)$ and $\mathcal{B}(K_S^0 \rightarrow \pi^+ \pi^-)$ [11]. For the $B^0 \rightarrow K^0 \pi^+ \pi^-$ branching fraction, the total charmless contribution to the Dalitz plot is measured (with charmed and charmonium resonances removed), including contributions from resonant charmless substructure.

The data used in this analysis were collected at the PEP-II asymmetric-energy $e^+ e^-$ storage ring with the *BABAR*

detector [12]. The *BABAR* detector consists of a double-sided five-layer silicon tracker, a 40-layer drift chamber, a Cherenkov detector, an electromagnetic calorimeter and a magnet with instrumented flux return. The data sample has an integrated luminosity of 210 fb^{-1} collected at the $Y(4S)$ resonance, which corresponds to $(231.8 \pm 2.5) \times 10^6 B\bar{B}$ pairs. It is assumed that the $Y(4S)$ decays equally to neutral and charged B -meson pairs. In addition, 21.6 fb^{-1} of data collected at 40 MeV below the $Y(4S)$ resonance were used for background studies.

The reconstruction of candidate B mesons combines two charged tracks and a K_S^0 candidate, with the K_S^0 being reconstructed from two oppositely charged tracks consistent with $\pi^+ \pi^-$. The B^0 decay vertex is reconstructed from the two charged tracks that were not daughters of the K_S^0 , with the requirements that the tracks originate from the beam-spot, have at least 12 hits in the drift chamber and have a transverse momentum greater than $100 \text{ MeV}/c$. K_S^0 candidates are required to have a reconstructed mass within $15 \text{ MeV}/c^2$ of the nominal K_S^0 mass [11], at least a 5 standard deviation separation between the B^0 decay vertex and its own decay vertex, and a cosine of the angle between the line joining the B^0 and K_S^0 decay vertices and the K_S^0 momentum vector greater than 0.999. To identify pions we use measurements of energy loss (dE/dx) in the tracking system, the number of photons detected by the Cherenkov detector and the corresponding Cherenkov angle. Candidate pions must fail the electron selection, which is based on dE/dx measurements, shower shape in the calorimeter, and the ratio of energy in the calorimeter to momentum in the drift chamber. Using simulated Monte Carlo (MC) events, we determine an approximate mean and width (σ) of the mass distribution for the resonances, and choose the resonance band to be $\pm 3\sigma$ from the mean. For the decay $B^0 \rightarrow K^{*+} \pi^-$ we require $0.776 < m_{K_S^0 \pi} < 1.010 \text{ GeV}/c^2$ and for $B^0 \rightarrow f_0 K_S^0$ we require $0.879 < m_{\pi^+ \pi^-} < 1.069 \text{ GeV}/c^2$.

The dominant source of background is continuum quark production ($e^+ e^- \rightarrow q\bar{q}$ where $q = u, d, s, c$). An event-shape variable, the cosine of the angle θ_T between the

thrust axis of the selected B candidate and the thrust axis of the rest of the event [12], is used to suppress this background. The distribution of $|\cos\theta_T|$ is strongly peaked towards unity for continuum background but is flat for signal events. The requirement $|\cos\theta_T| < 0.9$ reduces the relative amount of continuum background.

To separate signal events from the remaining background events, we use two kinematic variables and one event-shape variable. The first kinematic variable ΔE , is the difference between the center-of-mass (CM) energy of the B candidate and $\sqrt{s}/2$, where \sqrt{s} is the total CM energy of the e^+e^- beams. The second is the beam-energy-substituted mass $m_{\text{ES}} = \sqrt{(s/2 + \mathbf{p}_i \cdot \mathbf{p}_B)^2/E_i^2 - \mathbf{p}_B^2}$, where \mathbf{p}_B is the B momentum and (E_i, \mathbf{p}_i) is the four-momentum of the $Y(4S)$ in the laboratory frame. We require these variables to be in the ranges $|\Delta E| < 0.1$ GeV and $5.22 < m_{\text{ES}} < 5.29$ GeV/ c^2 . We construct a Fisher discriminant (\mathcal{F}) [13] using a linear combination of five event-shape variables: the cosine of the angle between the B -candidate momentum and the beam axis, the cosine of the angle between the B -candidate thrust axis and the beam axis, the zeroth and second angular moments of the energy flow about the thrust axis of the B [2], and the output of the B -flavor tagging algorithm, which uses the information from the other B [14]. This forms a more efficient Fisher discriminant than used in our previous measurement, Ref. [4].

Other B -meson decays can mimic a $K_S^0\pi^+\pi^-$ final state. MC events are used to identify the B decays that contribute background events to the data sample, and we use the available information on exclusive measurements [11,15] to find how many events from this background to expect in the data set. The largest B background is seen to come from quasi two-body decays including charmonium mesons such as $J/\psi K_S^0$, $\chi_{c0} K_S^0$ and $\psi(2S)K_S^0$. In these cases the charmonium meson decays to $\pi^+\pi^-$ or to $\mu^+\mu^-$ that are misidentified as pions. Most of these events are removed by vetoing the reconstructed $\pi^+\pi^-$ masses consistent with $3.04 < m_{\pi^+\pi^-} < 3.16$ GeV/ c^2 , $3.32 < m_{\pi^+\pi^-} < 3.51$ GeV/ c^2 and $3.63 < m_{\pi^+\pi^-} < 3.74$ GeV/ c^2 , identifying the J/ψ , χ_{c0} and $\psi(2S)$ mesons, respectively. From simulated data we estimate that 126 ± 8 $B^0 \rightarrow J/\psi K_S^0$ events and 6 ± 3 $B^0 \rightarrow \psi(2S)K_S^0$ events fall outside these vetoes, and these are included in the model. We veto events that are consistent with $B^0 \rightarrow D^-(\rightarrow K_S^0\pi^-)\pi^+$ by excluding those with $1.8 < m_{K_S^0\pi^-} < 1.91$ GeV/ c^2 . However, Monte Carlo simulation shows that 71 ± 8 $B^0 \rightarrow D^-(\rightarrow K_S^0\pi^-)\pi^+$ background events still remain, where the reconstructed D^+ mass falls outside the veto as a result of using a K_S^0 or a π from the other B decay in the event. Other incorrectly reconstructed charmed decays $B \rightarrow D^{(*)}X$ are also included in the model.

After the above selection criteria are applied, 12.4% of events have more than one candidate that satisfies the

selection criteria. In a signal MC study, selecting the candidate whose $\cos\theta_T$ value is closest to zero is found to select the true signal candidate in 69.2% of such events. These requirements result in a final sample size of approximately 80 000 events.

After all requirements, the largest charmless B background to the $B^0 \rightarrow K_S^0\pi^+\pi^-$ measurement is the decay $B^0 \rightarrow \eta' K_S^0$, $\eta' \rightarrow \rho^0(770)\gamma$, $\rho^0 \rightarrow \pi^+\pi^-$, which tends to peak in the signal region and which contributes 54 ± 19 events. Table I shows the B -background modes for the $B^0 \rightarrow K^{*\pm}\pi^\mp$ and $B^0 \rightarrow f_0 K_S^0$ channels. These events are effectively subtracted from the measured signal. To measure the nonresonant $B^0 \rightarrow K_S^0\pi^+\pi^-$, we select a region of the Dalitz plot believed to be free of resonances, ($3 < m_{\pi^+\pi^-} < 4$ GeV/ c^2 and $m_{K_S^0\pi^\pm} > 1.91$ GeV/ c^2). Backgrounds from other B decays and from continuum events are subtracted. Assuming a uniform nonresonant distribution in the Dalitz plane, we set an upper limit of 2.1×10^{-6} at a 90% confidence level on the nonresonant $B^0 \rightarrow K_S^0\pi^+\pi^-$ branching fraction. All other branching fractions are taken from Refs. [11,15].

We use an extended maximum likelihood fit to extract the signal yield for each of the channels being investigated. The likelihood function for N events is:

$$\mathcal{L} = \exp\left(-\sum_j N_j\right) \prod_i^N \left(\sum_{j=1}^M N_j P_j(\vec{x}_i)\right) \quad (2)$$

where i and j are integers, M is the number of hypotheses (signal, continuum background and B background), N_j is the number of events for the j th hypothesis determined by maximizing the likelihood function, and $P_j(\vec{x}_i)$ is a probability density function (PDF) evaluated using the vector \vec{x}_i , in this case m_{ES} , ΔE , and \mathcal{F} . Correlations between these variables are small for signal and continuum background hypotheses and the total PDF is a product $P_j(\vec{x}_i) = P_j(m_{\text{ES}}) \cdot P_j(\Delta E) \cdot P_j(\mathcal{F})$. However for B background, it is necessary to account for correlations observed between

TABLE I. The B -background modes for the channels $B^0 \rightarrow K^{*\pm}\pi^\mp$ and $B^0 \rightarrow f_0 K_S^0$. $B^0 \rightarrow \rho^0 K_S^0$ is included at a level consistent with Ref. [3]. K^{**} refers to heavier K^* resonances, e.g. $K_0^*(1430)$.

B -background Mode	Number Expected ($B^0 \rightarrow K^{*\pm}\pi^\mp$)	Number Expected ($B^0 \rightarrow f_0 K_S^0$)
$B^0 \rightarrow K^{*\pm}\pi^\mp$	—	5 ± 1
$B^0 \rightarrow f_0 K_S^0$	4 ± 1	—
$B^0 \rightarrow \rho^0 K_S^0$	5 ± 2	14 ± 4
$B^0 \rightarrow K^{**\pm}\pi^\mp$	23 ± 3	4 ± 1
Nonresonant	7 ± 1	5 ± 1
$B^0 \rightarrow D^\mp \pi^\pm$	16 ± 2	0
$B^0 \rightarrow \eta' K_S^0$	1 ± 1	19 ± 7
$B^0 \rightarrow J/\psi K_S^0$	6 ± 1	0

B. AUBERT *et al.*

PHYSICAL REVIEW D **73**, 031101 (2006)

m_{ES} and ΔE by using a two-dimensional PDF for these variables.

The parameters of the signal and B -background PDFs are determined from MC simulation and fixed in the fit, along with the B -background normalization. The continuum background parameters are allowed to vary in the fit, to help reduce systematic effects from this dominant event type. Sideband data (which lie in the region $0.1 < \Delta E < 0.3$ GeV and $5.22 < m_{ES} < 5.29$ GeV/ c^2) are used to model the continuum background PDFs. For the m_{ES} PDFs, a Gaussian distribution is used for signal and a threshold function [16] for continuum. For the ΔE PDFs, a sum of two Gaussian distributions with the same means is used for the signal and a first-order polynomial for the continuum background. Finally, for the \mathcal{F} PDFs, a sum of two Gaussian distributions with distinct means and widths is used for signal and a sum of two Gaussian distributions with the same means is used to model the continuum background. The Fisher discriminant distribution of the B backgrounds is modeled by an asymmetric Gaussian distribution that has different widths above and below the modal value. We use $B^0 \rightarrow D^- (\rightarrow K_S^0 \pi^-) \pi^+$ as a calibration mode since it exhibits a one-to-one signal to continuum background ratio, allowing the signal parameters in a fit to be floated. A fit to these data is used in order to quantify any corrections and uncertainties due to MC. These corrections are applied to the fits to the charmless data sample.

To extract the branching fractions for the decay modes $B^0 \rightarrow K^{*+} \pi^-$ and $B^0 \rightarrow f_0 K^0$ we use the relation

$$\mathcal{B} = \frac{N_{sig}}{2N_{B^0 \bar{B}^0} \varepsilon}, \quad (3)$$

where N_{sig} is the number of signal events fitted, ε is the signal efficiency obtained from MC and $N_{B^0 \bar{B}^0}$ is the total number of $B^0 \bar{B}^0$ pairs.

For the charmless $B^0 \rightarrow K^0 \pi^+ \pi^-$ branching fraction (and also for the nonresonant upper limit in the B -background studies above), it is necessary to account for the variation in efficiency, between approximately 5% and 40%, across the Dalitz plot and to know how the signal events are distributed across the Dalitz plot. To do this we assign to the j th event $\mathcal{W}_j = \sum_i V_{sig,i} P_i(\vec{x}_j) / \sum_k N_k P_k(\vec{x}_j)$ where $V_{sig,i}$ are the signal components of the covariance matrix obtained from the fit. This procedure projects out the signal distributions [17] shown in Figs. 1–4. The branching fraction is then calculated as $\mathcal{B} = \sum_j \mathcal{W}_j / (\varepsilon_j N_{B^0 \bar{B}^0})$, where ε_j is the efficiency, as a function of Dalitz plot position, simulated in small bins using high statistics MC.

Figure 1 shows the signal distributions for $B^0 \rightarrow K^0 \pi^+ \pi^-$ candidates and the distributions of events for all hypotheses. Figure 2 shows the signal distributions for both the $B^0 \rightarrow K^{*+} \pi^-$ and $B^0 \rightarrow f_0 K^0$ channels. The fitted signal yield and measured branching fraction are shown in

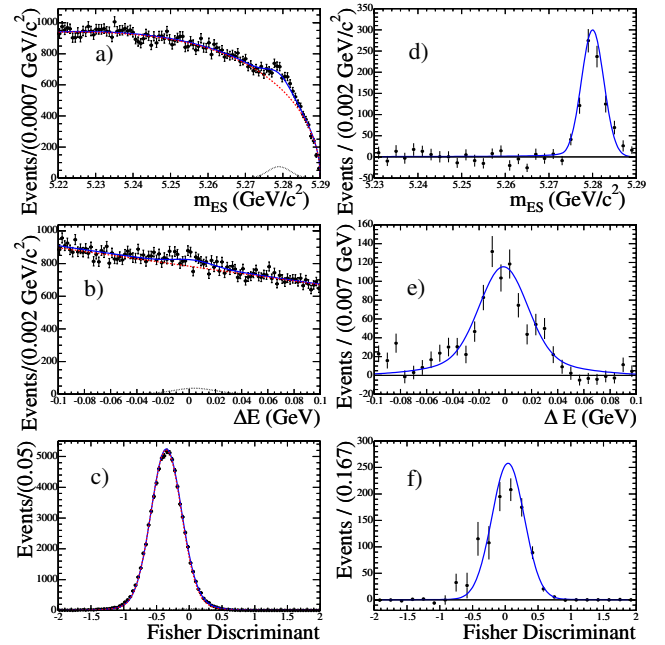


FIG. 1 (color online). Plots of the maximum likelihood fit to data for $B^0 \rightarrow K^0 \pi^+ \pi^-$ candidates. Plots (a)–(c) show the distributions of all events that pass the selection criteria for (a) m_{ES} (b) ΔE and (c) Fisher, with the solid (blue) line indicating the total model, the (red) dotted line indicating shape of the continuum background model and the (black) dashed line indicating the signal model. Plots (d)–(f) show the signal distributions for (d) m_{ES} , (e) ΔE and (f) Fisher, where the (black) circles are the signal distribution [17] and the solid (blue) curve is the signal PDF that was fitted in the maximum likelihood fit.

Table II for all the modes under study. The average efficiency for $B^0 \rightarrow K_S^0 \pi^+ \pi^-$ signal events is 16.8% and the continuum background yield is 79000 ± 280 events. Figure 3 shows the signal mass projections of $m_{K_S^0 \pi}$ and $m_{\pi^+ \pi^-}$ using $B^0 \rightarrow K^0 \pi^+ \pi^-$ candidates. The $m_{K_S^0 \pi}$ distribution clearly shows a peak at 0.9 GeV/ c^2 , corresponding to the K^{*+} (892) mass and there is a broad structure above 1 GeV/ c^2 that is the region where heavier kaon resonances can occur. The $m_{\pi^+ \pi^-}$ distribution shows evidence for resonance structure around 1 GeV/ c^2 that corresponds to the f_0 and a broader structure below this that may be attributed as the $\rho^0(770)$. Figure 4 shows the efficiency corrected signal distribution of the cosine of the helicity angle, θ_H , for $B^0 \rightarrow K^{*+} \pi^-$.

Table III shows the systematic uncertainties that are assigned to the branching fraction measurements. Control channels in data and MC are used to assign uncertainties due to pion tracking, particle identification, and K_S^0 reconstruction efficiency. To calculate uncertainties due to the fitting procedure, a large number of MC samples are generated from the fitted PDFs, containing the amounts of signal and continuum events that are measured in data and the number of B -background events that were anti-

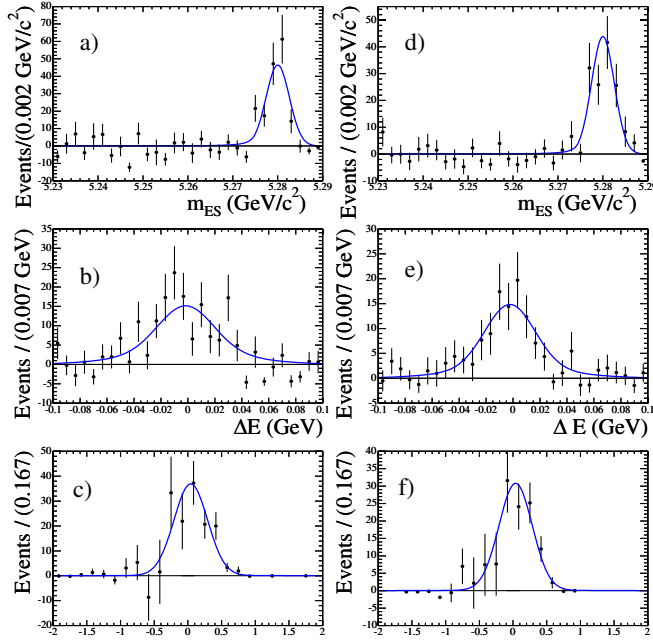


FIG. 2 (color online). Maximum likelihood fits for signal distributions. For $B^0 \rightarrow K^{*+} \pi^-$ the plots show (a) m_{ES} , (b) ΔE , and (c) the Fisher discriminant. The (black) circles are the signal distribution extracted from the data with the method of Ref. [17] and the solid curve is the signal PDF that resulted from the maximum likelihood fit. For $B^0 \rightarrow f_0 K^0$, plots show the distributions for (d) m_{ES} , (e) ΔE , and (f) the Fisher discriminant, in an analogous fashion.

pated for the data set, as explained above. The differences between the generated and fitted values using these samples are used to ascertain the sizes of any biases. Small biases of the order of a few percent are observed that are a consequence of small correlations between fit variables and are therefore assigned as systematic uncertainties.

TABLE II. Signal yields and branching fractions for $B^0 \rightarrow K^0 \pi^+ \pi^-$, $B^0 \rightarrow K^{*+} \pi^-$ and $B^0 \rightarrow f_0 K^0$ where the first uncertainty is statistical and where, in the case of the branching fraction measurements, the second uncertainty is systematic and any third uncertainty is due to possible interference effects. The efficiency of selecting $B^0 \rightarrow K^{*+} (\rightarrow K_S^0 \pi^+) \pi^-$ and $B^0 \rightarrow f_0 (\rightarrow \pi^+ \pi^-) K_S^0$ events was found to be 24% and 27% respectively, while the continuum background yields were 7300 ± 86 events and 13000 ± 110 events, respectively. The $B^0 \rightarrow K^{*+} \pi^-$ branching fraction takes into account that $\mathcal{B}(K^{*+} \rightarrow K^0 \pi^+) = 2/3$, assuming isospin symmetry.

Mode	Signal Events Yield	Branching Fraction ($\times 10^{-6}$)
$B^0 \rightarrow K^0 \pi^+ \pi^-$	860 ± 47	$43.0 \pm 2.3 \pm 2.3$
$B^0 \rightarrow f_0 (\rightarrow \pi^+ \pi^-) K^0$	120 ± 16	$5.5 \pm 0.7 \pm 0.6 \pm 0.3$
$B^0 \rightarrow K^{*+} \pi^-$	140 ± 19	$11.0 \pm 1.5 \pm 0.5 \pm 0.4$

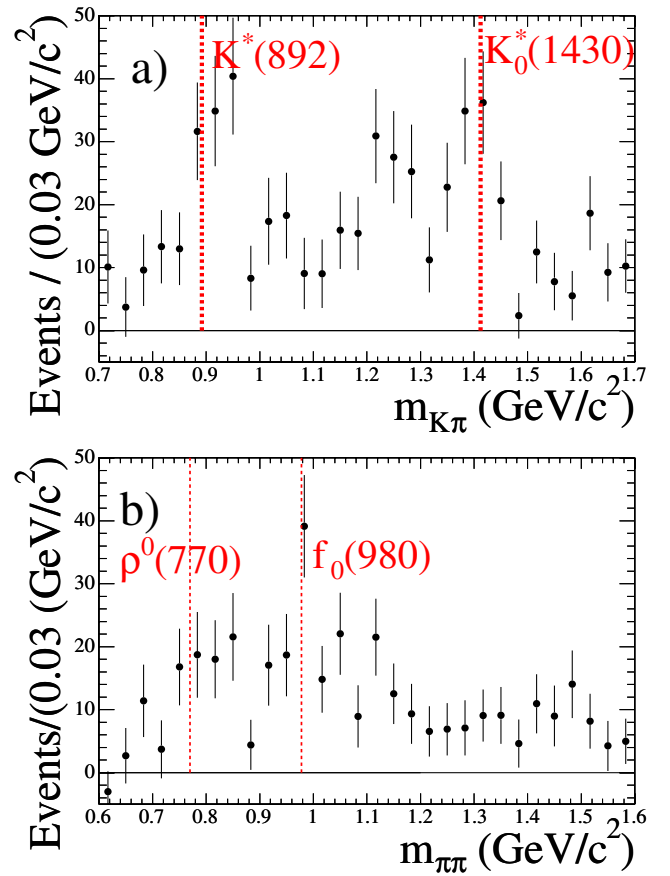


FIG. 3 (color online). (a) shows the $m_{K^0 \pi^-}$ signal distribution of $B^0 \rightarrow K^0 \pi^+ \pi^-$ candidates [17]. The one-dimensional distribution is obtained by merging $m_{K^0 \pi^+}^2$ and $m_{K^0 \pi^-}^2$ into one ($m_{K^0 \pi}^2$) by folding the Dalitz plane along the line corresponding to $m_{K^0 \pi^+}^2 = m_{K^0 \pi^-}^2$ in order to obtain the above $m_{K^0 \pi}$ mass distribution. (b) shows the $m_{\pi^+ \pi^-}$ signal distribution of $B^0 \rightarrow K^0 \pi^+ \pi^-$ candidates [17]. The dashed lines indicate the expected mass of the labeled resonances.

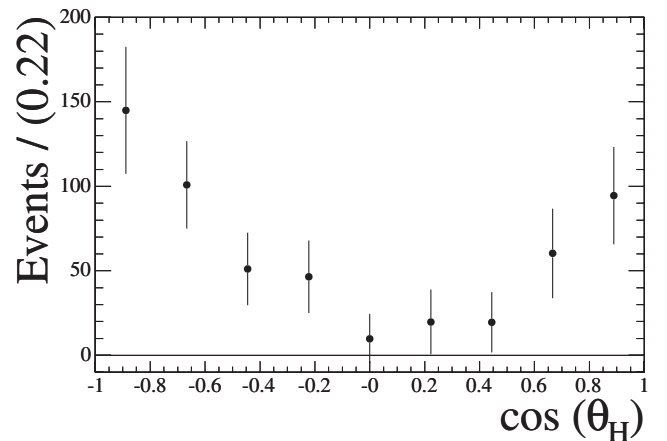


FIG. 4. Distribution of the efficiency corrected cosine of the helicity angle, θ_H , for $B^0 \rightarrow K^{*+} \pi^-$ signal events.

TABLE III. Summary of contributions to the systematic uncertainty in the branching fractions measurements of $B^0 \rightarrow K^0 \pi^+ \pi^-$, $B^0 \rightarrow K^{*+} \pi^-$ and $B^0 \rightarrow f_0 K^0$. The uncertainties are shown as a percentage of the measured branching fraction.

Error source	$B^0 \rightarrow K^0 \pi^+ \pi^-$ Error (%)	$B^0 \rightarrow f_0 K^0$ Error (%)	$B^0 \rightarrow K^{*+} \pi^-$ Error (%)
Particle ID	1.9	1.9	1.9
Tracking	1.6	1.6	1.6
K_S^0 efficiency	1.4	1.6	1.5
Fit Bias	1.7	6.1	2.6
PDF params.	0.1	0.1	0.3
B background	4.2	5.9	2.0
Efficiency	0.9	0.1	0.1
No. of $B\bar{B}$	1.1	1.1	1.1
TOTAL	5.4	9.1	4.5
Interference	-	4.7	4.0

The uncertainty of the B -background contribution to the fit is estimated by varying the measured branching fractions within their uncertainties. Each background is varied by $\pm 1\sigma$ [11] and the effect on the fitted signal yield is added as a contribution to the uncertainty. For $B^0 \rightarrow K^{*+} \pi^-$ there is an additional uncertainty in the B -background contributions due to the possible lineshapes of the $K_0^{*\pm}$ (1430), which can alter the amount of B background expected. In order to assign a systematic uncertainty, fits to data are performed using two parametrizations, a relativistic Breit–Wigner lineshape and the LASS parametrization [18]. The latter is a coherent sum of a relativistic Breit–Wigner and an effective range term, and is used in the analysis of $B^\pm \rightarrow K^\pm \pi^\mp \pi^\pm$ [19]. The uncertainty due to simulated PDFs is obtained from the channel $B^0 \rightarrow D^-(\rightarrow K_S^0 \pi^-) \pi^+$ and by varying the PDFs according to the precision of the parameters obtained from MC. In order to take correlations between parameters into account, the full correlation matrix is used when varying parameters. All PDF parameters that are originally fixed in the fit are then varied in turn and each difference from the nominal fit is combined and taken as a systematic uncertainty. The uncertainty in the efficiency is due to limited MC statistics, where over 1 000 000 MC events are generated for the decay $B^0 \rightarrow K^0 \pi^+ \pi^-$ and over 150 000 MC events are generated for the decays $B^0 \rightarrow K^{*+} \pi^-$ and $B^0 \rightarrow f_0 K_S^0$. The same uncertainty in the number of $B\bar{B}$ events is used for all channels.

For the quasi two-body modes, possible interference effects between the final state modes were investigated

by simulating the Dalitz plot using the measured branching fractions and random phases. The root-mean-squared of the distribution of the branching fraction is taken to be the uncertainty.

We measure the CP -violating charge asymmetry for the decay $B^0 \rightarrow K^{*+} \pi^-$ to be $\mathcal{A}_{K^* \pi} = -0.11 \pm 0.14 \pm 0.05$, where the first uncertainty is statistical and the second uncertainty is systematic. The charge asymmetry in the background is expected to be zero, as is the charge asymmetry in signal and background of the self-tagging decay $B^0 \rightarrow D^- \pi^+$. As a cross-check, these are measured to be -0.018 ± 0.009 , -0.013 ± 0.029 and 0.005 ± 0.031 respectively, where the uncertainties are statistical only.

The systematic uncertainty on $\mathcal{A}_{K^* \pi}$ is calculated by considering contributions due to track finding, particle identification, fit biases and B -background asymmetry uncertainties. Biases due to track finding and particle identification were found to be negligible. The fit-bias contribution to the systematic uncertainty is calculated using a large number of MC samples. The contribution from B background is calculated by varying the number of expected events within their uncertainties [11] and by assuming a conservative CP -violating asymmetry of ± 0.5 as there are no available measurements for these decays. The resulting systematic uncertainty on the asymmetry is measured to be ± 0.05 .

In summary, the branching fractions for $B^0 \rightarrow K^0 \pi^+ \pi^-$, $B^0 \rightarrow K^{*+} \pi^-$, and $B^0 \rightarrow f_0 (\rightarrow \pi^+ \pi^-) K^0$ decaying to a $K_S^0 \pi^+ \pi^-$ state are measured and all agree with previous measurements [2,4–6]. We measure the direct CP -violating parameter $\mathcal{A}_{K^* \pi}$ for the decay $B^0 \rightarrow K^{*+} \pi^-$, with no evidence of CP violation with the statistics used. These results supersede the previous results of the *BABAR* Collaboration [2,4].

We are grateful for the excellent luminosity and machine conditions provided by our PEP-II colleagues, and for the substantial dedicated effort from the computing organizations that support *BABAR*. The collaborating institutions wish to thank SLAC for its support and kind hospitality. This work is supported by DOE and NSF (USA), NSERC (Canada), IHEP (China), CEA and CNRS-IN2P3 (France), BMBF and DFG (Germany), INFN (Italy), FOM (The Netherlands), NFR (Norway), MIST (Russia), and PPARC (United Kingdom). Individuals have received support from CONACyT (Mexico), A. P. Sloan Foundation, Research Corporation, and Alexander von Humboldt Foundation.

- [1] N. Cabibbo, Phys. Rev. Lett. **10**, 531 (1963); M. Kobayashi and T. Maskawa, Prog. Theor. Phys. **49**, 652 (1973).
- [2] B. Aubert *et al.* (BABAR Collaboration), Phys. Rev. Lett. **94**, 041802 (2005).
- [3] B. Aubert *et al.* (BABAR Collaboration), hep-ex/0408079.
- [4] B. Aubert *et al.* (BABAR Collaboration), Phys. Rev. D **70**, 091103 (2004).
- [5] E. Eckhart *et al.* (CLEO Collaboration), Phys. Rev. Lett. **89**, 251801 (2002).
- [6] A. Garmash *et al.* (Belle Collaboration), Phys. Rev. D **69**, 012001 (2004).
- [7] M. Beneke and M. Neubert, Nucl. Phys. **B675**, 333 (2003); D. Du, J. Sun, H. Gong, D. Yang, and G. Zhu, Phys. Rev. D **65**, 094025 (2002); J. Sun, G. Zhu, and D. Du, Phys. Rev. D **68**, 054003 (2003); N. de Groot, W. N. Cottingham, and I. B. Whittingham, Phys. Rev. D **68**, 113005 (2003).
- [8] C. W. Chiang, M. Gronau, Z. Luo, J. L. Rosner, and D. A. Suprun, Phys. Rev. D **69**, 034001 (2004).
- [9] Z. Xiao, W. Li, L. B. Guo, and G. Lu, Eur. Phys. J. C **18**, 681 (2001).
- [10] B. Aubert *et al.* (BABAR Collaboration), Phys. Rev. Lett. **93**, 131801 (2004); Y. Chao *et al.* (Belle Collaboration), Phys. Rev. Lett. **93**, 191802 (2004).
- [11] S. Eidelman *et al.* (Particle Data Group), Phys. Lett. B **592**, 1 (2004).
- [12] B. Aubert *et al.* (BABAR Collaboration), Nucl. Instrum. Meth. A **479**, 1 (2002).
- [13] R. A. Fisher, Ann. Eugenics **7**, 179 (1936); G. Cowan, *Statistical Data Analysis* (Oxford University Press, New York, 1998) p. 51.
- [14] B. Aubert *et al.* (BABAR Collaboration), Phys. Rev. Lett. **95**, 041805 (2005)
- [15] The Heavy Flavor Averaging Group, <http://www.slac.stanford.edu/xorg/hfag/>.
- [16] H. Albrecht *et al.* (ARGUS Collaboration), Z. Phys. C **48**, 543 (1990).
- [17] M. Pivk and F. R. Le Diberder, Nucl. Instrum. Meth. A **555**, 356 (2005).
- [18] D. Aston *et al.* (LASS Collaboration), Nucl. Phys. **B296**, 493 (1988).
- [19] B. Aubert *et al.* (BABAR Collaboration), Phys. Rev. D **72**, 072003 (2005); A. Garmash *et al.* (Belle Collaboration), Phys. Rev. D **71**, 092003 (2005).